The protective effect of Artepillin C against lipid oxidation on model membranes

Wallance Moreira Pazin [1,*], Gilia Cristine Marques Ruiz [1], Marcelo José dos Santos [1], Pedro Henrique Benites Aoki [2], Amando Siuiti Ito [3] and Carlos José Leopoldo Constantino [1]

[1] São Paulo State University (UNESP), School of Technology and Applied Sciences, Presidente Prudente, SP, Brazil, 19060-900; wallance.pazin@unesp.br

[2] São Paulo State University (UNESP), School of Sciences, Humanities and Languages, Assis, SP, Brazil, 19806-900; pedro.aoki@unesp.br

[3] University of São Paulo (USP), Faculty of Philosophy, Sciences and Letters of Ribeirão Preto, Ribeirão Preto, SP, Brazil, 14040-901; amandosi@ffclrp.usp.br

* Corresponding author: Wallance Moreira Pazin

E-mail address: wallancepazin@gmail.com

Rua Roberto Simonsen, 305

19060-900, Presidente Prudente, Brazil

Tel.: +55 18 3229-5461

Abstract

Brazilian green propolis is a well-known therapeutic product, commonly used in folk medicine. Artepillin C is the major compound of Brazilian green propolis and has received considerable attention owing to its lipophilic affinity and antioxidant activity, enabling the use against lipid oxidation caused by free radicals, which is a first step before degenerative diseases. The protective effect of Artepillin C against lipid oxidation was evaluated here on models of lipid membranes based on Langmuir monolayers and giant unilamellar vesicles (GUVs) formed of 1,2-dioleoyl-sn-glycero-3-phosphocholine DOPC under oxidative stress induced by the photoactivated erythrosin. Our findings show that the lipophilic character of Artepillin C allows the donation of a hydrogen atom of the phenolic hydroxyl group to the lipid radical of both mono and bilayer, avoiding the formation of truncated aldehyde lipids, interrupting oxidative reactions mediated by reactive oxygen species (ROS), therefore playing a role as an antioxidant compound in the lipid environment. The affinity of Artepillin C for lipid structures, together with its antioxidant potential, preclude the lipid peroxidation caused by reactive species.

Keywords: Green propolis; Artepillin C; antioxidant activity; model membranes; erythrosine

1. Introduction

Human body is a complex system that develops its biological function with a high degree of organization, going from molecular levels up to process involving tissues, organs and members. However, the dynamic of metabolic process is not always successful. For instance, free radicals are released in the body, and, when in excess, have high reactivity with different molecules. It may trigger damages and mutation in the organism by the oxidative stress [1,2]. Therefore, improper molecular combination might be prejudicial to the metabolism, playing a role in the development of several deleterious effects in DNA, signaling proteins and cell membranes, leading to an early aging and to degenerative diseases, such as Alzheimer, Parkinson, atherosclerosis and cancer [3–5].

In the case of cell membranes, free radicals attack carbon-carbon double bonds present in the acyl chain, triggering lipid peroxidation [4,6]. It happens in three main stages: initiation, when free radicals removes the allylic hydrogen of acyl chain, creating the carbon-centered lipid radical (L•); propagation, starting from the moment that molecular oxygen reacts with L• generating peroxy-radical (LOO•). This reactive species captures a hydrogen from another lipid molecule in the membrane, creating a new L• that will react with O_2, turning this process cyclic (chain reaction) leading to the generation of degradation products, as aldehydes [7]. It can be avoided by the termination step, when antioxidant compounds take place donating their hydrogen atoms, ending the reaction [8]. A well-known example is the α-tocopherol (vitamin E), which donates a hydrogen atom to LOO• species, generating a radical compound that is able to react with another LOO•, therefore forming a non-radical termination product [7,8].

In a protective way, the biologic system has a defense mechanism involving redox agents aiming stabilization of free radicals by means of antioxidant action. It can be, for example, enzymes, vitamins (A, C and E) and natural pigments [1]. Although necessary,

this self-defense of the organism is not completely effective for the combat of oxidative stress in an eventual imbalance due to the excess of free radicals, mainly for the exposition of humans to the UV radiation, pollutants, tobacco smoke, heavy metals and polycyclic aromatic hydrocarbons [9–11]. In this perspective, despite the action of endogenous antioxidant agents, the introduction of exogenous compounds with high antioxidant capacity is capable of preventing or even regenerate damages caused by undesirable redox reaction.

Natural products rich in polyphenols, such phenolic acids, flavonoids, terpenes and aromatic aldehydes, identified as secondary metabolites, are often involved in the protection mechanisms to help in the adaptation of plants to the environment [12,13]. They have attracted attention mainly for presenting a large spectrum of pharmacological properties, including antioxidant activities against different types of free radicals [14]. Taking advantage of their benefits, bees collect secondary metabolites from the plant exudates for the protection of their hives against parasites and diseases, forming propolis [15]. Particularly in Brazil, green propolis is constituted of several secondary metabolites collected by *Apis mellifera* especially from *Baccharis dracunculifolia* [16]. To date, Brazilian green propolis is extensively consumed worldwide, especially in Asiatic countries, due to its several biological properties, including, besides antioxidant properties, antitumor, antimicrobial, anti-inflammatory activities [17–21]. Among the bioactive compounds, Artepillin C (ArtC) stands out since it is the major and the most biologically relevant compound of such Brazilian propolis [22,23], with a wide range of pharmacological properties, as reported above for Brazilian green propolis [23–25]. The high quality of propolis correlates to the amount of ArtC in its composition [18]. It is a simple phenolic acid derivative with two prenylated groups imparting hydrophobicity that ensure its affinity for lipophilic environment [26–28]. This feature correlates with the

success of applying ArtC as an antioxidant agent mainly for protection of cell membranes, since the hydroxyl group of aromatic ring is available for the redox process with the free radical via one-step hydrogen atom transfer [29]. Szliszka et al. have reported the radical-scavenging activity of ArtC against 1,1-diphenyl-2-picrylhydrazyl radical (DPPH) and 2,2′-Azinobis(3-ethylbenzothiazoline-6-sulfonic acid) radical cation ($ABTS^{\bullet+}$), with ED_{50} values 24.6 and 19.5 μM, respectively [23]. Massaeli et al. [30] reported the higher potential of antioxidant agents with lipophilic affinity instead of those with hydrophilic property against lipid peroxidation reaction, owed by the efficiency of transferring the hydrogen atom to the lipid radical directly in the cell membrane, leading rapidly to the end of the reaction by the production of a non-radical product. A recent published study performed by Sadžak et al. (2020) investigated the antioxidative potential of three different flavonols in both hipdrophilic and hydrophobic environments, suggesting that the protective effect of lipid bilayers upon oxidative stress, preserving the supramolecular and mechanical properties of the membrane, is dependent on the environment in which they are located [31].

As we shall demonstrate in this study, the lipophilic character of ArtC and its antioxidant capacity are able to interrupt oxidative reactions mediated by the photoactivated erythrosin B in a lipid environment. Langmuir monolayers and Giant Unilamellar Vesicles (GUVs) of 1,2-dioleoyl-sn-glycero-3-phosphocholine (DOPC) were used as bioinspired systems of cell membranes. DOPC imparts one carbon-carbon double-bond in each acyl chain, which is a target for reactive species. In general, ArtC avoids a fast membrane permeabilization and generates an area excess of the model membranes due to the production of hydroperoxides as a final step of its antioxidant action.

2. Materials and Methods

ArtC (3,5-diprenyl-4-hydroxycinnamic acid), isolated and purified (98.43%) from Brazilian green propolis, was purchased from Wako (Japan). 1,2-Dioleoyl-sn-glycerol-3-phosphocholine (DOPC) was purchased from Avanti Polar Lipids, Inc. (Alabaster, AL, USA) and used without further purification. Erythrosin, polyvinyl alcohol (PVA, M.W. 146.000 – 186.000 g/mol), HEPES, sodium chloride (NaCl), and the organic solvents (chloroform and methanol) of analytical grade were purchased from Sigma Chemical Co. (St. Louis, MO, USA). Aqueous solutions were obtained with ultrapure Milli-Q® water (resistivity 18.2 MΩ.cm, surface tension 72 mN/m, 25 °C). The molecular structures of ArtC, DOPC and erythrosin are displayed in Figure 1.

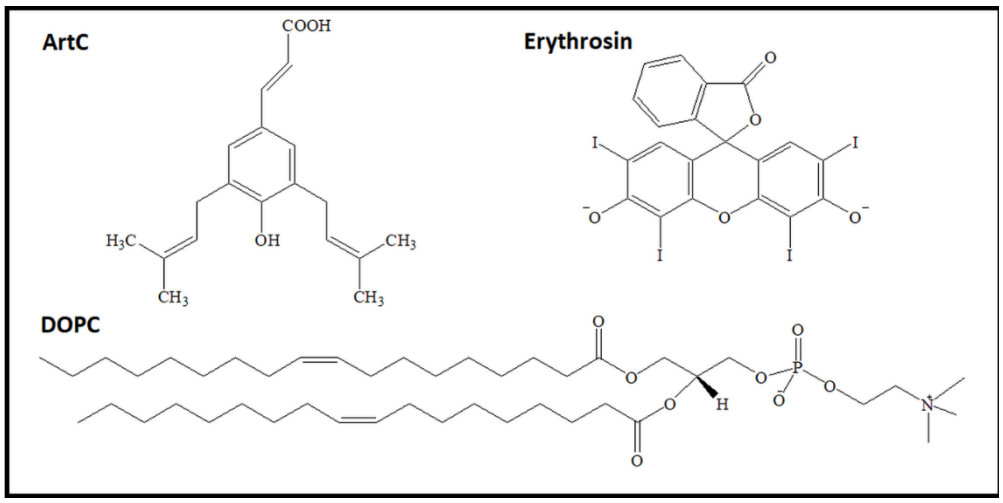

Figure 1. Molecular structures of Artepillin C, erythrosin and DOPC.

2.1. Surface pressure versus mean molecular area (π-A) isotherms

DOPC solution in chloroform (0.50 mg.mL^{-1}) was spread on a 150-cm² (length = 30.00 cm; width = 5.00 cm) Langmuir trough (KSV Instruments Ltd., Helsinki, Finland). Lipid monolayers were formed at the air/liquid interface with symmetrical compression

of the barriers at a constant rate of 10 mm/min, ten minutes after spreading DOPC solution onto the subphase, required for chloroform evaporation. Surface pressure (π) vs mean molecular area (Å) isotherms were obtained using a platinum plate as Wilhelmy sensor. The monolayers were compressed on buffer (HEPES buffer 10 mM, pH 7.4 and NaCl 150 mM) and buffer containing erythrosin (10 μM) or/and ArtC (10 μM). Light-irradiation was performed with green LED (530 nm – 50 W, BRIWAX FFG) placed 20 cm above the monolayer to monitor the surface pressure stability at a constant mean molecular area. A negative control was also acquired in dark, without any influence of either external or LED light. All isotherms were recorded in triplicate at 23 °C (room temperature).

2.2. Giant unilamellar vesicles (GUVs)

Giant unilamellar vesicles (GUVs) were assembled on a polyvinyl alcohol (PVA) film, as previously reported by Weinberger et al [32]. This method allows GUVs to swell avoiding ions interference and lipid oxidation that might happen when they are growth by the traditional electroformation method [33]. Briefly, a PVA solution (5% w/w) was initially prepared in milli-Q water at 90 °C and kept under stirring until complete solubilisation. 500 μL of the solution was then dropped on the bottom of a well (5 cm in diameter) and placed in an oven (~100 °C) for water evaporation. 20 μL of DOPC chloroform solution (1 mM) was then uniformly spread on PVA-coated well and left under vacuum for at least 1 hour. Afterwards, 1 mL of a sucrose solution (200 mM) prepared in HEPES buffer (150 mM NaCl, 10 mM HEPES) was added to the well, allowing GUVs to swell for 1h30min at room temperature. GUVs were piped from the PVA-coated well and stored in Eppendorf tubes. For microscope observation, 50 μL of GUVs suspensions were added to an eight-well polymer chamber (Ibidi, Munich,

Germany) containing 200 µL of iso-osmolar glucose-buffer solution with the desired concentration of ArtC and/or erythrosin. A negative control was performed by adding methanol (0.8% v/v) in the well, which was the necessary volume to reach the maximum concentration of ArtC in the glucose-buffer solution for this study. The osmolality of both sucrose and glucose solutions were checked using a freezing point Osmometer (Osmomat 3000 – Gonotec GmbH, Berlin, Germany). The vesicles settle at the bottom of the microscope-chamber owing to the density difference between glucose and sucrose, thus facilitating the observation. The experiments were performed in an inverted confocal microscope (Nikon C2/C2si Eclipse Ti-E, Kyoto, Japan), using a 40x air objective, NA 0.9, by means of phase contrast. The samples were irradiated using an excitation band filter (540/25) placed in the epi-fluorescence light path of a mercury lamp. The experiments were performed at least in triplicate, at 23 °C (room temperature) and the images were analyzed with ImageJ.

2.3. Statistical analysis

The experimental data were collected in triplicate, processed using OriginPro® 8.5 and evaluated by the analysis of standard deviation.

3. Results and discussion

3.1. π-A isotherms

The *π-A* isotherms obtained for DOPC monolayers on buffer (pH 7.4 and 150 mM NaCl) and buffer containing 10 µM of ArtC, erythrosin, and erythrosin + ArtC mixture are shown in Figure 2a.

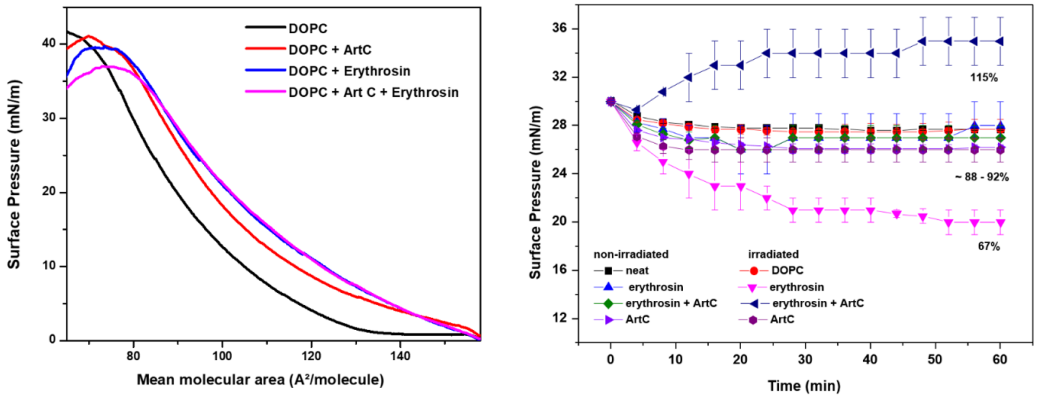

(**a**) (**b**)

Figure 2. a) π-A isotherms of DOPC Langmuir films at 23 °C on buffer (HEPES solution at 10 mM and pH 7.4 + 150 mM of NaCl; black line) and buffer containing 10 μM of ArtC (red line), 10 μM of erythrosin (blue line) and 10 μM of the ArtC and erythrosin mixture (magenta line); b) Surface pressure time dependence of irradiated and non-irradiated DOPC monolayer on buffer (HEPES solution at 10 mM and pH 7.4 + 150 mM of NaCl) and buffer containing 10 μM of ArtC, 10 μM of erythrosin and 10 μM of the ArtC and erythrosin mixture.

Both ArtC and erythrosin are not surface active [34,35] and cannot form Langmuir monolayers when in a mixture, as shown by the subsidiary experiment in Figure S1. Such compounds expand the π-A isotherms of DOPC, even at higher surface pressures, suggesting their interaction on the monolayers. We have confirmed in a previous study [34] a preferential adsorption of ArtC in the polar region of DPPC monolayers owing to the negative charge of the carboxyl group (COO^-), which form a stabilized intramolecular hydrogen bonding with the water molecules at the water/lipid interface. Considering that DPPC and DOPC share the same phosphatidyl head groups, it is likely that interactions of the same nature governs the ArtC adsorption on DOPC monolayers. Moreover, the less packed DOPC monolayers may have allowed deeper penetration of ArtC, resulting in larger expansion in the π-A isotherms, relatively to DPPC. Indeed, previous studies have shown ArtC embedded in deeper regions of lipid vesicles in fluid state [28], which can

226 be related to cohesive van der Waals interaction between the ring moiety of ArtC bearing
227 two prenyl groups with the unsaturated acyl chains.

228 The dianionic erythrosin is driven to DOPC monolayers mainly by attractive
229 electrostatic interactions with the cationic choline groups, with penetration into the
230 chains, as previously reported [35]. Compared to ArtC, erythrosin causes larger expansion
231 on DOPC monolayers, which can be notice by the higher right-shift in the π-A isotherms
232 (Figure 2a). The latter is not only related to the larger size (e.g. the presence of conjugated
233 rings) of erythrosin but also to the additional negative charge that can increase the
234 electrostatic repulsion with the anionic phosphate in the lipid heads, hindering the
235 monolayer packing. Such features can be also confirmed by the π-A isotherm formed in
236 presence of the ArtC + erythrosin mixture, which resembles the one containing only
237 erythrosin, i.e., despite ArtC interacting with DOPC monolayer, the larger effects in
238 occupied area per lipid molecule is predominantly caused by the physicochemical
239 properties of erythrosin towards lipid monolayer interaction. Although the insertion of
240 the molecules at the liquid/air interface reflects in a shift of the DOPC monolayers to
241 larger areas, it does not cause significant changes in overall monolayer elasticity, as
242 shown in Supporting Information (SI 2), preserving the shapes and profiles of the
243 isotherms.

244 Additional analysis on the collapse pressure shows a slightly decreased upon
245 erythrosin adsorption, supporting the electrostatic repulsion previously proposed. ArtC +
246 erythrosin mixture further decreased the collapse pressure, confirming the monolayer
247 instability in relation to DOPC on buffer and buffer containing ArtC or erythrosin.

248 The stability of irradiated and non-irradiated DOPC monolayers on buffer and buffer
249 containing ArtC, erythrosin, and erythrosin + ArtC mixture were monitored at 30 mN/m,
250 which is believed to correspond to the lateral pressures of cell membranes [36]. Upon

reaching the target pressure, the surface area was kept constant and further modification in the pressure was followed over time, as displayed in Figure 2b. In all the non-irradiated monolayers, the surface pressure stabilizes at 27 ± 1 mN/m along 1 hour, after reaching 30mN/m. This decrease in surface pressure could be related to the monolayer stabilization after a sudden stop of the barriers. Light irradiation of DOPC monolayer containing erythrosin decreased the surface pressure to 20 mN/m (~ 67%), which did not occur for monolayers without its presence. It is already known that erythrosin presents high quantum yield of singlet oxygen ($^1O_2$) upon irradiation [37]. This reactive oxygen species (ROS) is generated by the energy transfer from the excited states of erythrosin to the molecular oxygen of the environment. The hydroperoxide generation has been shown to be the main outcome of the $^1O_2$ reaction with the chain unsaturations, which subsequently disturb the hydrophilic-hydrophobic balance of the lipid membranes [35]. Moreover, the propagation of the oxidative reaction can result in the cleavage of the chains at the unsaturation site. The photoactivated erythrosin can attack the chain unsaturation, or previously formed hydroperoxides, by contact-dependent reactions that result in truncated lipid aldehydes [38]. The latter are solubilized by the subphase, reducing the amount of material at the lipid interface and, consequently, decreasing the surface pressure of the monolayer as observed in this study. On the other hand, the surface pressure of irradiated DOPC monolayer on erythrosin + ArtC mixture increased to 34.5 mN/m (115%), suggesting a protective action of ArtC against oxidation and, consequently, avoiding the production of truncated lipid aldehydes. It is likely that a hydrogen atom of the phenolic hydroxyl group is donated to the lipid radical [29], blocking the propagation of the oxidative reaction. Therefore, the oxidative reaction may have terminated with the hydroperoxide generation owed to the antioxidant potential of ArtC [7,8], which correlates directly to the increase the mean molecular area of the phospholipid, resulting

in the overall surface pressure increase of the monolayer. An illustrative representation of the involved processes is displayed in Figure 3.

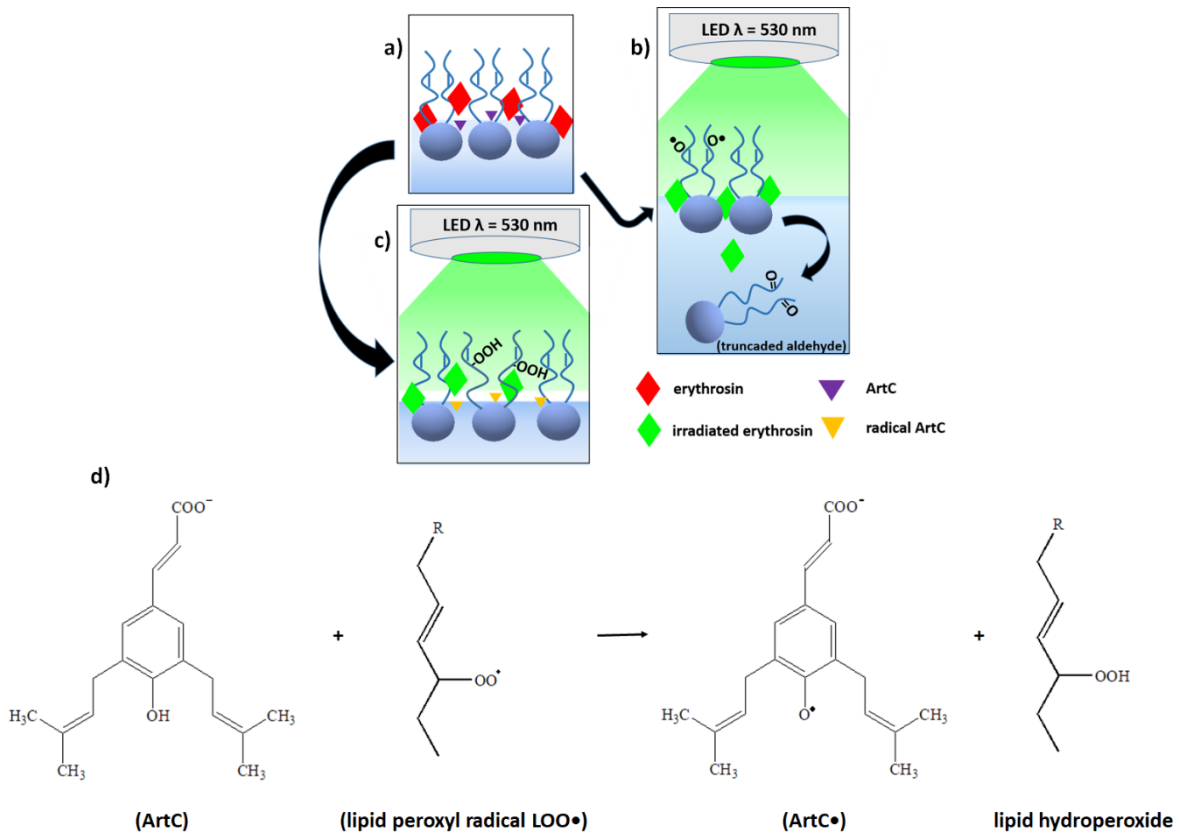

Figure 3. Schematic illustration of the presence of ArtC and erythrosin towards lipid monolayer (a); photoinduced erythrosin, in absence of AtC, generating truncated aldehyde by the cleavage of DOPC chains (b); protective action of ArtC against oxidation by the generation of hydroperoxide lipids as a termination step (c); reaction representing a hydrogen atom donation from ArtC to the lipid peroxyl radical (LOO•), generating lipid hydroperoxide (d).

3.2. GUVs as model membranes

Qualitative analysis was performed with GUVs in order to better understand how ArtC plays antioxidant activity against photoproducts in lipophilic environment, particularly in a system that represents cell size and plasma membrane curvature. GUVs immersed in 10 μM of both erythrosin and ArtC were not affect (data not shown), as

292 expected from previous reported data [34,39]. While light-irradiation at 540 ± 25 nm did
293 not produce any visible modification on GUVs immersed in 100 µM ArtC solution (see
294 Supporting Information SI 3), lipid bilayers are significantly affected in erythrosin, as
295 shown in Figure 4. Fluctuations are observed right after the beginning of the irradiation
296 and 10 seconds later the surface area of the GUVs is increased, with no loss of contrast.
297 Membrane permeabilization is observed after 150 seconds with the pore opening and the
298 contrast fades away at ca. 300 seconds of irradiation, remaining with the same shape for
299 the whole time of observation (ca. 3600 s – data not shown). Lipid hydroperoxidation in
300 the first seconds explains the surface area increase of GUVs, resulting from $^1O_2$ ene
301 reaction with alkenes containing allylic hydrogens [35], although the same could not be
302 observed at the beginning of surface pressure analysis in Langmuir monolayer probably
303 due to the barrier stabilization in the first 5 minutes. The pore opening and membrane
304 permeabilization is result of the cleavage of the lipid chains triggered by contact-
305 dependent reactions [38], which is consistent to the data on Langmuir monolayers.
306 Indeed, the formation of truncated lipid aldehydes favors water penetration by an increase
307 in the lipid-lipid distance, causing the pore opening in the membrane and further
308 permeabilization [38,40].

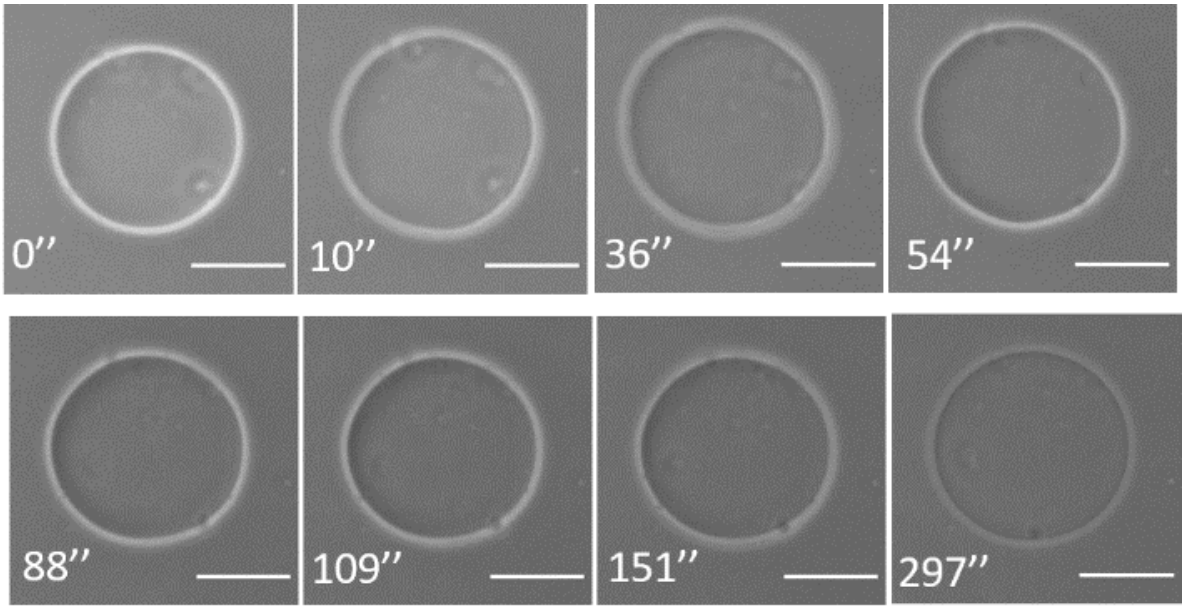

Figure 4. Phase contrast images acquired for DOPC GUVs suspended in 10 μM erythrosin solution, under irradiation at 540 ± 25 nm. Scale bar: 5 μm.

The protective action of ArtC against lipid oxidation was evaluated by irradiating GUVs immersed in a solution containing 10 μM of both erythrosin and ArtC. Although the same photo-oxidation effects of GUVs in erythrosin solution (Figure 4) are noted in Figure 5, ArtC has retarded the sequence of events. For instance, membrane fluctuations and surface area increase were noticed after ca. 36 seconds and ca. 54 seconds, respectively. Buds are created after ca. 88 seconds as result of the excess of area generated and the phase contrast is almost completely lost after ca. 530 seconds irradiation. This sequence of events is further delayed with the increase of ArtC concentration (Figure S4), suggesting an increased protective effect against photosensitized species. Antioxidant compounds such as ArtC plays a role in the termination step of lipid peroxidation by a donation of the hydrogen atom to LOO• species, generating hydroperoxides and nonradical products by the reaction of antioxidant radical with another LOO• [8], as already shown in the representation of the reaction between ArtC and the lipid peroxyl radical in Figure 2d. It most likely explains the reason that took the GUV to maintain for

a longer time both surface membrane fluctuation and area excess caused by the presence of hydroperoxide groups. Moreover, ArtC possibly apart its antioxidant activity avoiding contact-dependent mechanism, acting directly against erythrosin photoproduct, although the permeabilization can be observed after GUVs recover its spherical shape, remaining with the same shape even after a long time of observation.

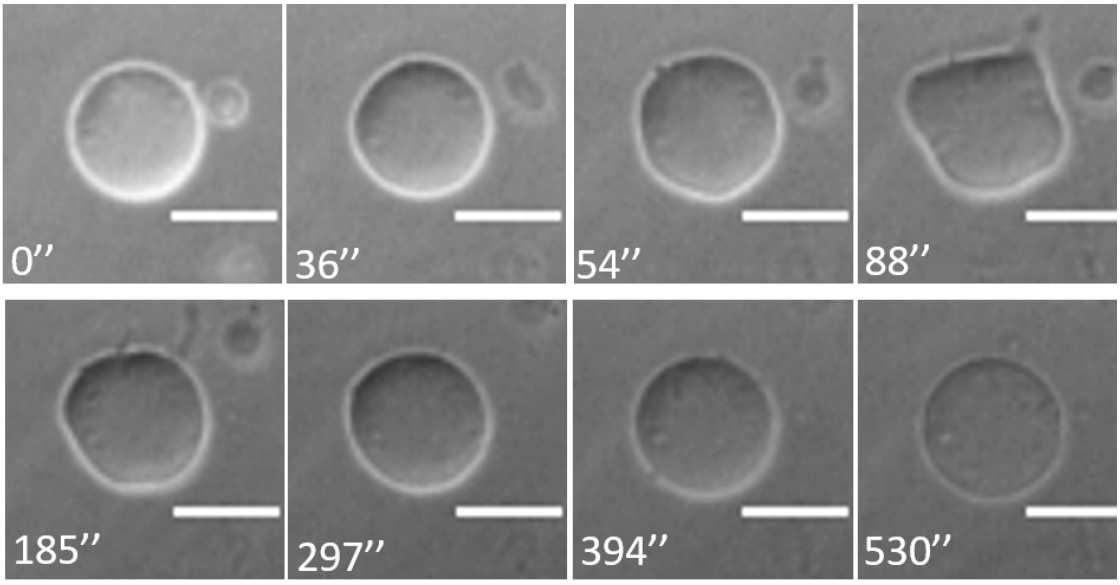

Figure 5. Phase contrast images acquired for DOPC GUVs suspended in a solution containing 10 μM of both erythrosin and ArtC. Scale bar: 5 μm.

4. Conclusions

The affinity of ArtC for lipophilic environment, correlated to its particular structure that ensure its antioxidant activity, allow it to act as a protective compound against lipid oxidation caused by the reactive species that attack the double bounds of acyl chains in unsaturated lipids. It was confirmed by means of time-dependent surface-pressure stability of lipid monolayers and analysis in the morphology of GUVs, formed of DOPC. The first reveals that the increase in the surface pressure results from the hydroperoxides

formed at the interface, while the same effect occur for GUVs, resulting in the increase in the membrane surface area. Both results suggest that ArtC donates a hydrogen atom of the phenolic hydroxyl group to the lipid radical that is formed by the contact-dependent reaction between photosensitized erythrosin and the double-bond of acyl chains of DOPC in the monolayer. Therefore, instead the fast formation of truncated aldehyde lipids, ArtC plays a role in the termination step of lipid peroxidation generating hydroperoxides, which increase both lipid per area in the DOPC monolayer and surface area of DOPC GUVs. It is worth to mention that, as already published recently regarding the antitumor action of ArtC [24], a subject of our current investigation aims to correlate and contribute the results obtained from the studies performed with model membranes with the antioxidant activity of ArtC in healthy cellular models, evidencing its action in the cell membrane.

Acknowledgments: We thank INEO and FAPESP (2016/09633-4 and 2018/22214-6) for funding support. GCMR is grateful to CAPES for a PhD fellowship, received during the development of this work. CJLP and ASI are recipients of a CNPq research grant (304100/2018-8 and 305771/2016-7, respectively). PHBA thanks FAPESP (2018/16713-0) for his research grant.

Conflicts of Interest: The authors declare no conflict of interest.

References

1. Birben, E.; Sahiner, U.M.; Sackesen, C.; Erzurum, S.; Kalayci, O. Oxidative Stress and Antioxidant Defense. *World Allergy Organ. J.* **2012**, *5*, 9–19, doi:10.1097/WOX.0b013e3182439613.
2. Kruk, J.; Aboul-Enein, H.Y.; Kładna, A.; Bowser, J.E. Oxidative stress in

biological systems and its relation with pathophysiological functions: the effect of physical activity on cellular redox homeostasis. *Free Radic. Res.* **2019**, *53*, 497–521, doi:10.1080/10715762.2019.1612059.

3. Jiang, T.; Sun, Q.; Chen, S. Oxidative stress: A major pathogenesis and potential therapeutic target of antioxidative agents in Parkinson's disease and Alzheimer's disease. *Prog. Neurobiol.* **2016**, *147*, 1–19, doi:10.1016/j.pneurobio.2016.07.005.
4. Su, L.J.; Zhang, J.H.; Gomez, H.; Murugan, R.; Hong, X.; Xu, D.; Jiang, F.; Peng, Z.Y. Reactive Oxygen Species-Induced Lipid Peroxidation in Apoptosis, Autophagy, and Ferroptosis. *Oxid. Med. Cell. Longev.* **2019**, *2019*, doi:10.1155/2019/5080843.
5. Muthuraman, A.; Rishitha, N.; Paramakrishnan, N.; Mahendran, B.; Ramesh, M. Role of Lipid Peroxidation Process in Neurodegenerative Disorders. In *Lipid Peroxidation Research*; IntechOpen, 2020; Vol. i, p. 13.
6. Griendling, K.K.; Touyz, R.M.; Zweier, J.L.; Dikalov, S.; Chilian, W.; Chen, Y.-R.; Harrison, D.G.; Bhatnagar, A. Measurement of Reactive Oxygen Species, Reactive Nitrogen Species, and Redox-Dependent Signaling in the Cardiovascular System. *Circ. Res.* **2016**, *119*, e39–e75, doi:10.1161/RES.0000000000000110.
7. Mostafa Abd El-Aal, H.A.H. Lipid Peroxidation End-Products as a Key of Oxidative Stress: Effect of Antioxidant on Their Production and Transfer of Free Radicals. In *Lipid Peroxidation*; InTech, 2012.
8. Ayala, A.; Muñoz, M.F.; Argüelles, S. Lipid Peroxidation: Production, Metabolism, and Signaling Mechanisms of Malondialdehyde and 4-Hydroxy-2-Nonenal. *Oxid. Med. Cell. Longev.* **2014**, *2014*, 1–31, doi:10.1155/2014/360438.
9. Pizzino, G.; Irrera, N.; Cucinotta, M.; Pallio, G.; Mannino, F.; Arcoraci, V.; Squadrito, F.; Altavilla, D.; Bitto, A. Oxidative Stress: Harms and Benefits for

Human Health. *Oxid. Med. Cell. Longev.* **2017**, *2017*, doi:10.1155/2017/8416763.

10. Jeng, H.A.; Pan, C.-H.; Diawara, N.; Chang-Chien, G.-P.; Lin, W.-Y.; Huang, C.-T.; Ho, C.-K.; Wu, M.-T. Polycyclic aromatic hydrocarbon-induced oxidative stress and lipid peroxidation in relation to immunological alteration. *Occup. Environ. Med.* **2011**, *68*, 653–658, doi:10.1136/oem.2010.055020.
11. Wooten, J.B.; Chouchane, S.; McGrath, T.E. Tobacco Smoke Constituents Affecting Oxidative Stress. In *Cigarette Smoke and Oxidative Stress*; Springer Berlin Heidelberg: Berlin, Heidelberg, 2006; pp. 5–46.
12. Isah, T. Stress and defense responses in plant secondary metabolites production. *Biol. Res.* **2019**, *52*, 39, doi:10.1186/s40659-019-0246-3.
13. Pereira, R.J.; Cardoso, M.D.G. Vegetable secondary metabolites and antioxidants benefits. *J. Biotechnol. Biodivers.* **2012**, *3*, 146–152.
14. Shan, S.; Huang, X.; Shah, M.H.; Abbasi, A.M. Evaluation of Polyphenolics Content and Antioxidant Activity in Edible Wild Fruits. *Biomed Res. Int.* **2019**, *2019*, 1–11, doi:10.1155/2019/1381989.
15. Neves Cruz, J.; Gomes da Silva, A.; Almeida da Costa, W.; Simone Cajueiro Gurgel, E.; Eduardo Oliveira Campos, W.; Campos e Silva, R.; Ene Chaves Oliveira, M.; Pedro da Silva Souza Filho, A.; Santiago Pereira, D.; Gomes Silva, S.; et al. Volatile Compounds, Chemical Composition and Biological Activities of Apis mellifera Bee Propolis. In *Essential Oils - Bioactive Compounds, New Perspectives and Applications*; IntechOpen, 2020.
16. Rodrigues, D.M.; De Souza, M.C.; Arruda, C.; Pereira, R.A.S.; Bastos, J.K. The Role of *Baccharis dracunculifolia* and its Chemical Profile on Green Propolis Production by Apis mellifera. *J. Chem. Ecol.* **2020**, *46*, 150–162, doi:10.1007/s10886-019-01141-w.

418 17. Salatino, A. Brazilian Red Propolis: Legitimate Name of the Plant Resin Source.
419 *MOJ Food Process. Technol.* **2018**, *6*, doi:10.15406/mojfpt.2018.06.00139.
420 18. Zhang, C. ping; Shen, X. ge; Chen, J. wei; Jiang, X. sen; Wang, K.; Hu, F. liang
421 Artepillin C, is it a good marker for quality control of Brazilian green propolis?
422 *Nat. Prod. Res.* **2017**, *31*, 2441–2444, doi:10.1080/14786419.2017.1303697.
423 19. Mariano, L.N.B.; Arruda, C.; Somensi, L.B.; Costa, A.P.M.; Perondi, E.G.;
424 Boeing, T.; Mariott, M.; da Silva, R. de C.M.V. de A.F.; de Souza, P.; Bastos, J.K.;
425 et al. Brazilian green propolis hydroalcoholic extract reduces colon damages
426 caused by dextran sulfate sodium-induced colitis in mice. *Inflammopharmacology*
427 **2018**, doi:10.1007/s10787-018-0467-z.
428 20. Wang, K.; Jin, X.; Li, Q.; Sawaya, A.C.H.F.; Le Leu, R.K.; Conlon, M.A.; Wu, L.;
429 Hu, F. Propolis from Different Geographic Origins Decreases Intestinal
430 Inflammation and Bacteroides spp. Populations in a Model of DSS-Induced
431 Colitis. *Mol. Nutr. Food Res.* **2018**, doi:10.1002/mnfr.201800080.
432 21. Chan, G.C.-F.; Cheung, K.-W.; Sze, D.M.-Y. The Immunomodulatory and
433 Anticancer Properties of Propolis. *Clin. Rev. Allergy Immunol.* **2013**, *44*, 262–273,
434 doi:10.1007/s12016-012-8322-2.
435 22. Machado, B.A.S.; Silva, R.P.D.; Barreto, G. de A.; Costa, S.S.; Silva, D.F. da;
436 Brandão, H.N.; Rocha, J.L.C. da; Dellagostin, O.A.; Henriques, J.A.P.; Umsza-
437 Guez, M.A.; et al. Chemical Composition and Biological Activity of Extracts
438 Obtained by Supercritical Extraction and Ethanolic Extraction of Brown, Green
439 and Red Propolis Derived from Different Geographic Regions in Brazil. *PLoS One*
440 **2016**, *11*, e0145954, doi:10.1371/journal.pone.0145954.
441 23. Szliszka, E.; Mertas, A.; Czuba, Z.P.; Król, W. Inhibition of Inflammatory
442 Response by Artepillin C in Activated RAW264.7 Macrophages. *Evidence-Based*

443 *Complement. Altern. Med.* **2013**, *2013*, 1–11, doi:10.1155/2013/735176.
444 24. Kobal, M.B.; Pazin, W.M.; Bistaffa, M.J.; Constantino, C.J.L.; Toledo, K.A.;
445 Aoki, P.H.B. Correlating Artepillin C cytotoxic activity on HEp-2 cells with
446 bioinspired systems of plasma membranes. *Mater. Sci. Eng. C* **2020**, *112*, 110943,
447 doi:10.1016/j.msec.2020.110943.
448 25. Veiga, R.S.; De Mendonça, S.; Mendes, P.B.; Paulino, N.; Mimica, M.J.; Lagareiro
449 Netto, A.A.; Lira, I.S.; López, B.G.-C.; Negrão, V.; Marcucci, M.C. Artepillin C
450 and phenolic compounds responsible for antimicrobial and antioxidant activity of
451 green propolis and *Baccharis dracunculifolia* DC. *J. Appl. Microbiol.* **2017**, *122*,
452 911–920, doi:10.1111/jam.13400.
453 26. Pazin, W.M.; Olivier, D. da S.; Vilanova, N.; Ramos, A.P.; Voets, I.K.; Soares,
454 A.E.E.; Ito, A.S. Interaction of Artepillin C with model membranes. *Eur. Biophys.*
455 *J.* **2017**, *46*, 383–393, doi:10.1007/s00249-016-1183-5.
456 27. Pazin, W.M.; Vilanova, N.; Voets, I.K.; Soares, A.E.E.; Ito, A.S. Effects of
457 artepillin C on model membranes displaying liquid immiscibility. *Brazilian J.*
458 *Med. Biol. Res.* **2019**, *52*, doi:10.1590/1414-431x20198281.
459 28. Camuri, I.J.; da Costa, A.B.; Ito, A.S.; Pazin, W.M. pH and Charge Effects Behind
460 the Interaction of Artepillin C, the Major Component of Green Propolis, With
461 Amphiphilic Aggregates: Optical Absorption and Fluorescence Spectroscopy
462 Studies. *Photochem. Photobiol.* **2019**, *95*, 1345–1351, doi:10.1111/php.13128.
463 29. Nakanishi, I.; Uto, Y.; Ohkubo, K.; Miyazaki, K.; Yakumaru, H.; Urano, S.;
464 Okuda, H.; Ueda, J.I.; Ozawa, T.; Fukuhara, K.; et al. Efficient radical scavenging
465 ability of artepillin C, a major component of Brazilian propolis, and the
466 mechanism. *Org. Biomol. Chem.* **2003**, *1*, 1452–1454, doi:Doi 10.1039/B302098c.
467 30. Massaeli, H.; Sobrattee, S.; Pierce, G.N. The importance of lipid solubility in

antioxidants and free radical generating systems for determining lipoprotein peroxidation. *Free Radic. Biol. Med.* **1999**, *26*, 1524–1530, doi:10.1016/S0891-5849(99)00018-0.

31. Sadžak, A.; Mravljak, J.; Maltar-Strmečki, N.; Arsov, Z.; Baranović, G.; Erceg, I.; Kriechbaum, M.; Strasser, V.; Přibyl, J.; Šegota, S. The Structural Integrity of the Model Lipid Membrane during Induced Lipid Peroxidation: The Role of Flavonols in the Inhibition of Lipid Peroxidation. *Antioxidants* **2020**, *9*, 430, doi:10.3390/antiox9050430.

32. Weinberger, A.; Tsai, F.C.; Koenderink, G.H.; Schmidt, T.F.; Itri, R.; Meier, W.; Schmatko, T.; Schröder, A.; Marques, C. Gel-assisted formation of giant unilamellar vesicles. *Biophys. J.* **2013**, *105*, 154–164, doi:10.1016/j.bpj.2013.05.024.

33. Stein, H.; Spindler, S.; Bonakdar, N.; Wang, C.; Sandoghdar, V. Production of isolated giant unilamellar vesicles under high salt concentrations. *Front. Physiol.* **2017**, *8*, 1–16, doi:10.3389/fphys.2017.00063.

34. Pazin, W.M.; Ruiz, G.C.M.; Oliveira, O.N. de; Constantino, C.J.L. Interaction of Artepillin C with model membranes: Effects of pH and ionic strength. *Biochim. Biophys. Acta - Biomembr.* **2019**, *1861*, 410–417, doi:10.1016/j.bbamem.2018.11.008.

35. Aoki, P.H.B.; Morato, L.F.C.; Pavinatto, F.J.; Nobre, T.M.; Constantino, C.J.L.; Jr., O.N.O. Molecular-Level Modifications Induced by Photo-Oxidation of Lipid Monolayers Interacting with Erythrosin. *Langmuir* **2016**, *32*, 3766–3773, doi:10.1021/acs.langmuir.6b00693.

36. Mostofsky, D.I.; Yehuda, S.; Salem Jr., N. *Fatty acids: Physiological and Behavioral Functions*; 2001;

493 37. Pellosi, D.S.; Batistela, V.R.; Souza, V.R. de; Scarminio, I.S.; Caetano, W.; Hioka,
494 N. Evaluation of the photodynamic activity of Xanthene Dyes on Artemia salina
495 described by chemometric approaches. *An. Acad. Bras. Cienc.* **2013**, *85*, 1267–
496 1274, doi:10.1590/0001-3765201395412.
497 38. Bacellar, I.O.L.; Baptista, M.S. Mechanisms of Photosensitized Lipid Oxidation
498 and Membrane Permeabilization. *ACS Omega* **2019**, *4*, 21636–21646,
499 doi:10.1021/acsomega.9b03244.
500 39. Aoki, P.H.B.; Schroder, A.P.; Constantino, C.J.L.; Marques, C.M. Bioadhesive
501 giant vesicles for monitoring hydroperoxidation in lipid membranes. *Soft Matter*
502 **2015**, *11*, 5995–5998, doi:10.1039/C5SM01019E.
503 40. Almeida, A.M.; Oliveira, O.N.; Aoki, P.H.B. Role of Toluidine Blue-O Binding
504 Mechanism for Photooxidation in Bioinspired Bacterial Membranes. *Langmuir*
505 **2019**, *35*, 16745–16751, doi:10.1021/acs.langmuir.9b03045.
506